*Available online www.jsaer.com*

***Journal of Scientific and Engineering Research*, 2018, 5(5):622-631**

**Research Article**

**ISSN: 2394-2630**
**CODEN(USA): JSERBR**

# Trace Elements Geochemistry of Nigde (Turkey) Antimony Deposits

**Sinan ALTUNCU*, Ali TÜMÜKLÜ, F. Zafer ÖZGÜR**

Niğde Omer Halisdemir University, Engineering Faculty, Geological Engineering Department, Turkey

**Abstract** Nigde Massif is the southest part of the CACC (Central Anatolian Crystalline Complex) which is composed of magmatic and metamorphic rocks. Within the massif is antimony mineralization of epithermal origin. According to the trace element geochemistry results of Çamardı (Niğde-Turkey) Sb mineralization. Hierarchical clusters are observed from the dendrograms for trace elements each other, indicating relatively high independency for each cluster. For Sb ore samples, Cd, Sn, Hf, Pb, Sr, In, I, Se, Te, Cs, Ni, Br, Te, Bi, Cu and As are very well correlated with each other and form a cluster which association with Rb, Tl, Nb, Mo, Th,Co, Zr, Zn, Hg, Ga, Ge and Y. La, Ce and W cluster joined only much later. Cd, Sn, Hf, Pb, In, I, Se, Te, Cs, Ni, Br, Te, Bi, Cu and As form the first cluster; Cd, Sn, Hf, Pb, In, I, Se, Te, Cs, Ni, Br, Te, Bi, Cu and As associated as the second cluster and La, Ce and W form the third cluster.

**Keywords** Antimony, Trace elements, Geochemistry, Nigde

## 1. Introduction

Anatolia is known as an economically important metallogenic province in the Alpine–Himalayan Belt [1]. The Tethyan Eurasian Metallogenic Belt (TEMB; [2]) extending from Western Europe through Anatolia to Iran is one of the world's major metal producing belts hosting many volcanogenic massive sulfide, porphyry-type (copper–gold and copper–molybdenum), low- and high-sulfidation epithermal (gold and gold–silver), mesothermal (lead, zinc, copper), and skarn (iron–copper, lead–zinc)-type deposits. The TEMB formed because of the convergence and collision of the Indian, Arabian and African tectonic plates with the Eurasian tectonic plate [3].Turkey antimony deposits are located in the Kütahya (Simav, Gediz), İzmir (Ödemiş), Tokat (Turhal), Nigde (Camardi, Gümüşler), Balıkesir (İvrindi Susurluk) Bursa (İnegöl) and Bilecik (Söğüt) provinces (Figure 1). The antimonite mineralizations in the Niğde Massif have an important place in Turkish mining. There are many Sb ± Hg, Sb + Hg, Sb ± Hg ± W and Hg ± Sb ore minerals that have been operated in the area in the past. The most important ones are Rasih-lhsan Sb + Hg ± W occurrences, Armutlar Tepe and Sinirsi Tepe Sb ± Hg occurrences, Ekinlik Tepe and Mehmetler Yurdu Sivrisi Tepe Hg ± Sb mineralizations [4]. The largest amount of ore production was conducted in the Rasih-İhsan occurrences [5,6], among these minerals operated by galleries and cuttings until 1980's.Antimony mineralizations associated with Üçkapılı granitoid cutting the Gümüşler, Kaleboynu and Aşıgediği formations in the Niğde massif between Niğde and Çamardı are investigated. The Nigde Massif is an isolated crystalline dome near the inner-Tauride suture in Central Turkey and represents the southern most part of the Central Anatolian Crystalline Complex (CACC, [7]), which includes the Kırşehir and Akdağ Massifs in the north. It is bounded on the east by the sinistral Ecemiş Fault (Tertiary) and on the South by the Ulukışla sedimentary basin. So far, there are many geological based researches in the region. These studies generally can be divided into three groups. The first is the studies carried out to determine the basic geological features of the region [8-9-10-11-12]. The second group especially belongs to the Sb ± Sn ± W ± Hg mineralization in the region [13-14-15]. The third group is related to environmental geochemistry [16-17].

In this study, mineralogical-petrographical investigation and geochemical characteristics of ore samples taken from the Madsan Sb mineralization in Niğde Massif have been discussed. The results of the trace elements in the geochemical analyzes were grouped and compared with the values of the Üçkapılı granitoids in the massif, and differences and similarities were tried to be revealed.

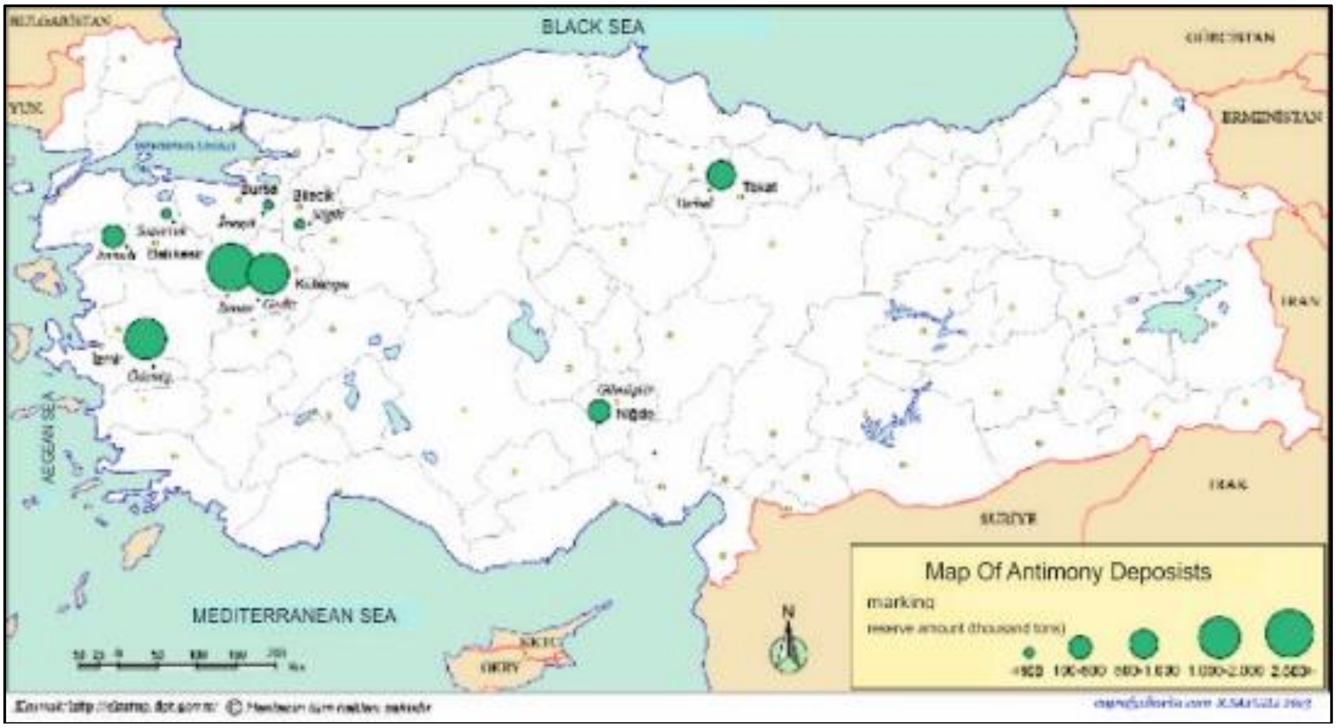


*Figure 1: The geographical distribution of Turkey antimony deposits*

## 2. Geological Setting

The Niğde massif, located at the southern tip of the CACC (Central Anatolian Crystaline Complex), isa structural dome comprised of a core that primarily consists of high-grade metasedimentary rocks (including migmatite) that record upper amphibolite facies metamorphism and, in the deepest structural units, partial melting [10-18]. These basement rocks are Gümüşler Formation, Kaleboynu Formation and Aşıgediği Formation in stratigraphic order from old to young. In the study area, the local stratigraphy starts with the Paleozoic Gümüşler Formation which is made of mostly gneiss, amphibolite, marble and quartzite. During pre-LateCretaceous time, the Sineksizyayla gabbro intruded into the Gümüşler Formation. The unit underwent deformation and metamorphism together with the Niğde Group rocks, probably during the emplacement of the Üçkapılı Granitoid. Kaleboynu Formation is dominated by marble, with alternations of quartzite, gneiss and amphibolite. Aşıgediği Formation which covers almost half of the Niğde Massif consists mainly of marbles with intercalations of gneiss, quartzite and amphibolite. All these units are cut by the crustally derived Late Cretaceous Üçkapılı two-mica granite and its vein rocks with a thickness of 30-100 cm like numerous aplite, micropegmatite and pegmatite dykes which are distributed mainly in the Gümüşler Formation. The dykes are also locally present in the Kaleboynu and Aşıgediği Formations. They are the late associates of the granitic intrusions and intrude all the units of the Niğde Group, including the main granitoid stock around Üçkapılı village. Incesu Ignimbrite covers unconformably all the units of the Niğde Massif and is covered by the Quaternary alluvial deposits [19] (Figure 2). Granitoids are abundant in the Niğde Massif, intruding the high-grade metamorphic series. The main intrusion is the Üçkapılı granite [20], exposed from the center of the massif to the northeast. Smaller exposures of granitoid, similar in appearance to the main body, are also wide spread further northwest and south. The most common facies is a two-mica granite. Analyses on samples from several small intrusions in the northwest document that the magma was per aluminous, with a high initial Sr ratio (0.7104 ± 0.0009) [20]. U-Pb geochronology on a sample from the main body shows that most zircons include an inherited core [18]. These features indicate that Üçkapılı-type magmas originate from partial melting of the continental crust [18-20]. Pressure conditions during emplacement were probably around 3–4 kbar [10]. The Üçkapılı Granitoid usually shows very weak ductile fabrics. It is locally associated with a dense array of dikes with variable orientations, crosscutting at a high angle the foliation of the metamorphic rocks. These features might suggest that the emplacement of the Üçkapılı Granitoid was post-tectonic. The main body, however, has been identified as a late-kinematic intrusion, recording the same shearing deformation as its host rocks [12].

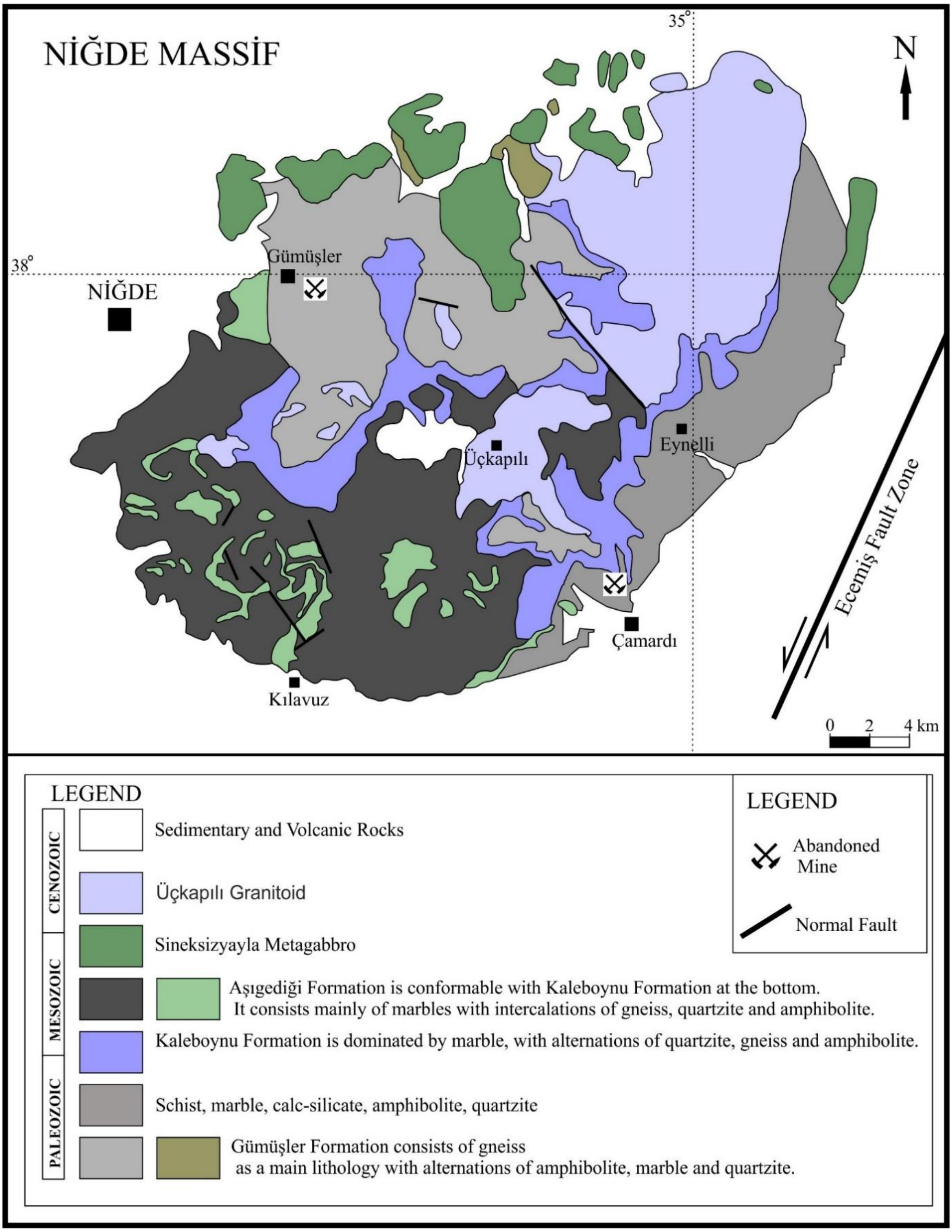


*Figure 2: Generalized geological map of the Niğde Massif [18].*

**3. Madsan Sb Mineralization in Nigde Massif**

The Sb mineralization in the region is located in a wide area between Gümüşler and Çamardı (Nigde). Gümüşler Sb deposits are located in Armutlar Tepe, Sinirsi Tepe, Ekinlik Tepe, Mehmetler Yurdu Sivrisi Tepe, Çamardı deposits are located in Gediz Plateau and Madsan (east of Tandırlık ridge).The deposists had been operated by open pit and underground mining operation methods until 1980. Today, there are no ore areas mined in the region. The mineralization in the study area are located in discontinuities in the Gümüşler, Kaleboynu and Aşıgediği formations. The Sb mineralization is classified as "simple antimony"-type (also known as quartz-stibnite, syntectonic stibnite and mesothermal Sb-Au). This corresponds to the granite-related vein-type (and replacement) deposits in the classification of Dill (2010) [21] and as epithermal using Lindgren's (1933) [22] definition. The mineral assemblage of the Gumusler (Nigde-Turkey) deposit includes scheelite, barite, stibnite, gold (up to 37.3 ppm) together with cinnabarite and Sb-sulphosalts. The Sb–Hg–W and Ba–Sb ore bodies are fracture bound with disseminations and veinlets of Hg–Sb in brecciated zones. The mineralization is genetically related to postmagmatic fluids associated with the Cenomanian granitic magmatism [4].The Üçkapılı Granodiorite that intruded the Gümüşler Metamorphics crops out as small patches around the Madsan antimony deposit [13].

The Madsan Sb deposit is hosted by white marbles, calc-silicate marbles and sericitized gneisses of the Gümüşler Metamorphics of the Central Anatolian Metamorphics [23]. The Madsan mineralizations are (1) quartz-stibnite veins along the marble-gneiss contacts and at the crests of folded calc-silicate marbles, (2) quartz-pyrite-stibnite veins along the foliation planes of the gneisses, (3) quartz-pyrite veins along the foliation and fracture planes of the gneisses, and (4) quartz veins along the marble-gneiss contacts [13].

In this study, Sb ore samples taken from Madsan abandoned open pit mine (Figure 3) were studied. The samples are quartz vein bearing samples in classifications made by Kuşcu and Erler (1999) [13].

*Figure 3: Abandoned open pit mine*

The outer surfaces of the samples are of varying colors, ranging from redish to yellowish and brownish due to the alteration. Stibnite ($Sb_2S_3$) and cinnabar (HgS) were identified as ore minerals in the ore samples. (Figure 4). Stibnite mineralization was detected in the form of veins and veinlets as fracture and crack fillers. Ore vein thicknesses are generally between 0.5-10 cm (Figure 5, a-b-c) and are located in quartzite or altered quartzites. The thickness of the veinlets is reduced to 100 µm (Figure 6, a-b).The stibnites are generally anhedral, with no evidence of deformation except pressure lamellae (Figure 6).The edges of stibnite is surrounded by a thin belt-shaped mercury from cinnabar minerals. Generally, cinnabars are 10-20 µm thick.


*Figure 4: Stibnite ($Sb_2S_3$) and cinnabar (HgS) were identified as ore minerals in the ore samples.*

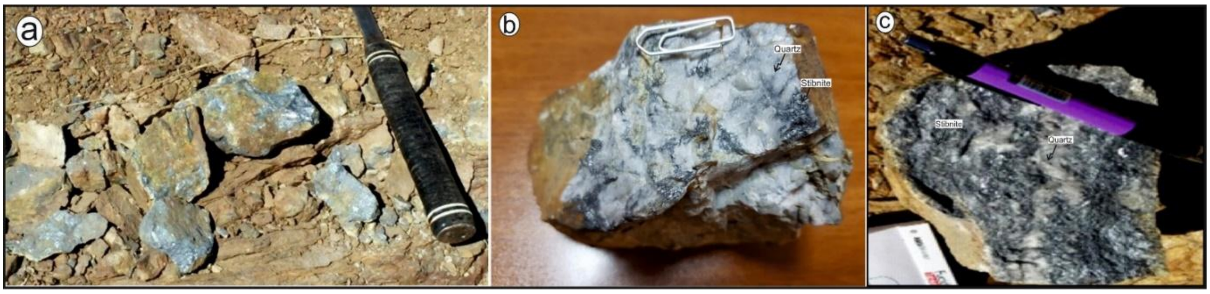


*Figure 5: a-b-c. Ore veins seen as fracture and crack filling*

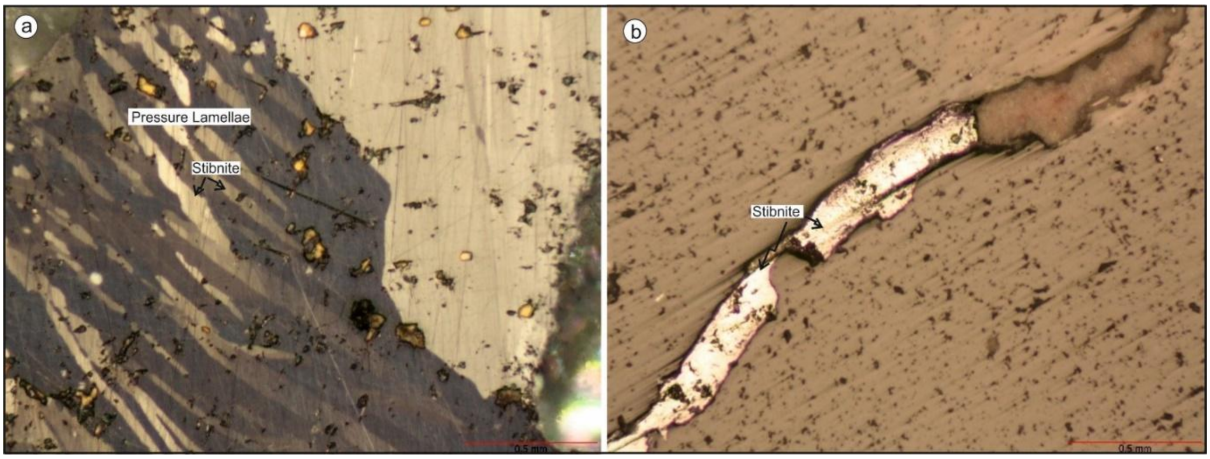


*Figure 6: a- pressure lamellae b- crack filling*

## 4. Geochemistry

The main oxides ($SiO_2$, $Al_2O_3$, $Fe_2O$, MgO, CaO, $Na_2O$, $TiO_2$, $P_2O_5$, MnO and $SO_3$) were determined by XRF method and the trace elements (Co, Ni, Zn, Ga, Ge, As, Sc, Br, Rb, Sr, Y, Zr, Nb, Mo, Cd, In, Sn, Sb, Te, I, Cs, Ba, La, Ce, Hf, TA, W, Au, Hg, Tl, Pb, Bi and Th) were determined by ICP-MSmethod on four ore samples selected from the study area.The results are shown in Table 1. These results were evaluated statistically.

**Table 1:** Geochemical analysis results

| | 1 | 2 | 3 | 4 |
|---|---|---|---|---|
| **Major oxides** | | | | |
| $SiO_2$ | 68.42 | 41.44 | 88.06 | 56.42 |
| $Fe_2O_3$ | 0.98 | 1.65 | 0.01 | 0.01 |
| $Al_2O_3$ | 0.94 | 0.45 | 1.05 | 0.168 |
| MgO | 0.28 | 0.51 | 0.30 | 0.02 |
| CaO | 1.18 | 0.26 | 3.28 | 41.04 |
| $SO_3$ | 15.02 | 31.47 | 5.90 | 0.12 |
| $Na_2O$ | 0.51 | 0.49 | 0.07 | 0.08 |
| $K_2O$ | 0.48 | 0.52 | 0.25 | 0.01 |
| $TiO_2$ | 0.04 | 0.14 | 0.01 | 0.02 |
| $P_2O_5$ | 0.03 | 0.08 | 0.15 | 0.01 |
| MnO | 0.01 | 0.01 | 0.03 | 0.06 |
| LOI | 1.13 | 1.73 | 0.72 | 2.73 |
| Total | 89.02 | 78.75 | 99.83 | 100.68 |
| **Trace Elements (ppm)** | | | | |
| Co | 62.00 | 30.10 | 47.70 | 17.60 |
| Ni | 19.60 | 20.70 | 7.80 | 2.20 |
| Cu | 37.80 | 41.80 | 1.10 | 1.20 |
| Zn | 95.80 | 14.20 | 8.60 | 0.50 |
| Ga | 8.30 | 2.40 | 4.60 | 3.30 |
| Ge | 8.20 | 2.20 | 2.60 | 1.00 |
| As | 1827.00 | 2249.00 | 163.30 | 31.60 |
| Se | 0.90 | 1.00 | 0.90 | 0.50 |
| Br | 5.70 | 6.40 | 2.00 | 0.70 |
| Rb | 18.30 | 11.30 | 6.60 | 1.00 |
| Sr | 1414.00 | 12.40 | 279.00 | 125.20 |
| Y | 7.40 | 2.30 | 1.00 | 8.80 |
| Zr | 30.00 | 17.00 | 22.20 | 6.90 |
| Nb | 16.00 | 12.00 | 5.00 | 4.20 |
| Mo | 17.00 | 13.00 | 5.00 | 3.50 |
| Cd | 5.10 | 82.00 | 4.10 | 1.70 |
| In | 5.20 | 39.00 | 6.90 | 1.10 |
| Sn | 33.60 | 705.00 | 1.80 | 1.20 |
| Sb | 3034.00 | 228800.00 | 311.80 | 123.20 |
| Te | 20.00 | 24.00 | 15.60 | 1.40 |
| I | 22.00 | 64.00 | 52.30 | 2.30 |
| Cs | 104.00 | 95.00 | 76.90 | 3.80 |
| Ba | 116400.00 | 144.00 | 25530.00 | 141.10 |
| La | 27.00 | 21.00 | 93.10 | 8.90 |
| Ce | 24.00 | 29.00 | 64.00 | 11.00 |
| Hf | 9.80 | 29.80 | 2.80 | 3.30 |
| Ta | 11.00 | 14.40 | 4.10 | 3.30 |
| W | 16.90 | 123.90 | 660.00 | 43.10 |
| Au | <0.1 | <0.1 | 14.60 | <0.1 |
| Hg | 714.90 | 15.50 | 4.20 | 2.50 |
| Tl | 36.80 | 20.40 | 11.50 | 2.30 |
| Pb | 49.00 | 196.10 | 13.30 | 4.10 |
| Bi | 7.30 | 10.80 | 1.50 | 1.00 |
| Th | 3.50 | 2.20 | 0.90 | 1.10 |

**5. Conclusions**

**Hierarchical Cluster Analysis**

Three clusters are observed from the dendrograms (Figure 7) for trace elements each other, indicating relatively high independency for each cluster. For Sb ore samples, Cd, Sn, Hf, Pb, Sr, In, I, Se, Te, Cs, Ni, Br, Ta, Bi, Cu and As are very well correlated with each other and form a cluster which association with Rb, Tl, Nb, Mo, Th, Co, Zr, Zn, Hg, Ga, Ge and Y is shown in Figure 7. La, Ce and W cluster joined only much later. Cd, Sn, Hf, Pb, In, I, Se, Te, Cs, Ni, Br, Te, Bi, Cu and As form the first cluster; Cd, Sn, Hf, Pb, In, I, Se, Te, Cs, Ni, Br, Te, Bi, Cu and As associated as the second cluster and La, Ce and W form the third cluster.

**Interelement Relationships**

Table 2 shows the positive and negative relationships of the elements in the correlation matrix distributions of the analyzed trace elements. Correlation coefficient does not explain the causal relations between variables. According to the calculated correlation coefficient, the linear relation values are is very weak between 0.00-0.25, weak between 0.26-0.49, moderate between 0.50-0.69, strong between 0.70-0.89 and very strong between 0.90-1.00 [24].

Trace elements belonging to the Üçkapılı granitoid were published byKurt et. al (2013). The following results were obtained when comparing the average values of the trace elements of the Üçkapılı granitoid with the values of Cu, Pb, Sr, Ba, Ta, Cs, Zn, Ga, Rb, Th, Nb, Zr and Y trace elements obtained in this study (Table 3). For the evaluated elements (Cu, Pb, Sr, Ba, Ta, Cs, Zn, Ga, Rb, Th, Nb, Zr and Y), the average of the values found in the Üçkapılı granite and ore samples was taken into account.In this sense, mean values of Cu, Pb, Sr, Ba, Ta and Cs show an increase in Sb ore samples.However, the mean values of Zn, Ga, Rb, Th, Nb, Zr and Y show an increase in the Üçkapılı granitoid.In this evaluation, all the elements which have increased in Sb ores (Cu, Pb, Sr, Ba, Ta and C) are in the first group in hierarchical cluster analysis, and elements which have increased in granitoid (Zn, Ga, Rb, Th, Nb, Zr and Y) is in the second group.

It has been found that the solutions which are separated from the Üçkapılı granitoid in the epithermal phase and caused the Sb mineralization in the region are enriched in Cu, Pb, Sr, Ba, Ta and Cs and consumed significantly in terms of Zn, Ga, Rb, Th, Nb, Zr and Y when compared to granitoid (Table 3).

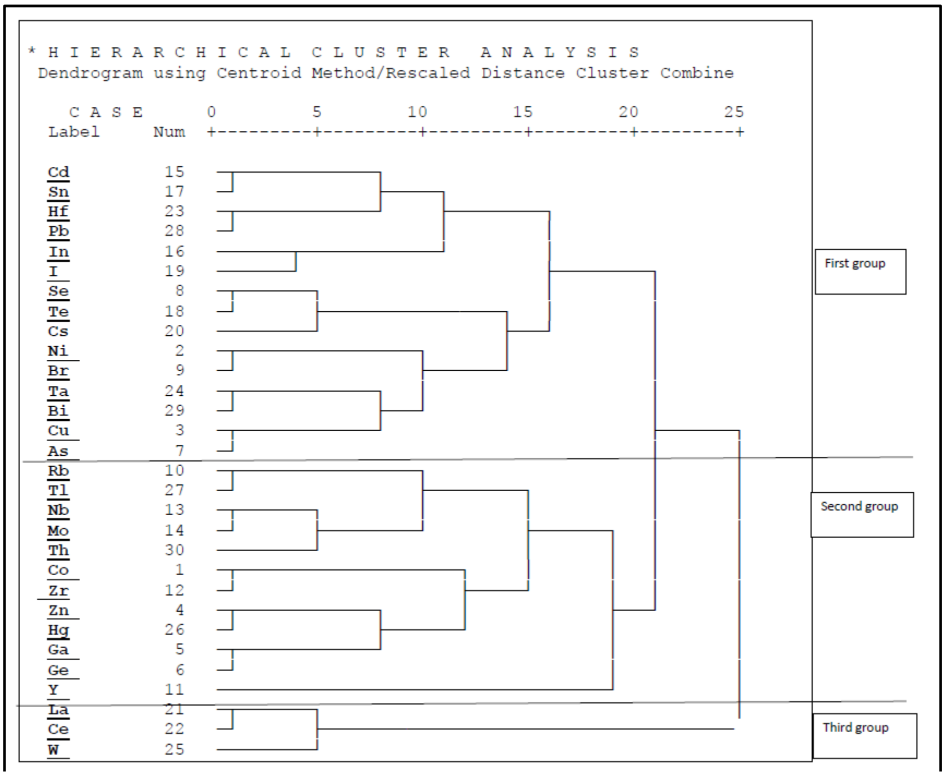


*Figure 7: Dendogram of trace elements of ores*

**Table 2:** Coefficient correlation between the trace elements on Çamardı Sb mineralizations.

| | Co | Ni | Cu | Zn | Ga | Ge | As | Se | Br | Rb | Sr | Y | Zr | Nb | Mo | Cd | In | Sn | Sb | Te | I | Cs | Ba | La | Ce | Hf | Ta | W | Hg | Tl | Pb | Bi | Th | U |
|---|---|---|---|---|---|---|---|---|---|---|---|---|---|---|---|---|---|---|---|---|---|---|---|---|---|---|---|---|---|---|---|---|---|---|
| Co | 1,00 | | | | | | | | | | | | | | | | | | | | | | | | | | | | | | | | | |
| Ni | 0,51 | 1,00 | | | | | | | | | | | | | | | | | | | | | | | | | | | | | | | | |
| Cu | 0,35 | 0,97 | 1,00 | | | | | | | | | | | | | | | | | | | | | | | | | | | | | | | |
| Zn | 0,81 | 0,62 | 0,60 | 1,00 | | | | | | | | | | | | | | | | | | | | | | | | | | | | | | |
| Ga | 0,87 | 0,31 | 0,24 | 0,92 | 1,00 | | | | | | | | | | | | | | | | | | | | | | | | | | | | | |
| Ge | 0,88 | 0,61 | 0,55 | 0,99 | 0,94 | 1,00 | | | | | | | | | | | | | | | | | | | | | | | | | | | | |
| As | 0,32 | 0,97 | 1,00 | 0,54 | 0,18 | 0,50 | 1,00 | | | | | | | | | | | | | | | | | | | | | | | | | | | |
| Se | 0,60 | 0,82 | 0,66 | 0,34 | 0,18 | 0,41 | 0,71 | 1,00 | | | | | | | | | | | | | | | | | | | | | | | | | | |
| Br | 0,44 | 1,00 | 0,98 | 0,58 | 0,25 | 0,56 | 0,99 | 0,79 | 1,00 | | | | | | | | | | | | | | | | | | | | | | | | | |
| Rb | 0,80 | 0,90 | 0,84 | 0,88 | 0,70 | 0,89 | 0,81 | 0,72 | 0,87 | 1,00 | | | | | | | | | | | | | | | | | | | | | | | | |
| Sr | 0,83 | 0,42 | 0,39 | 0,97 | 0,98 | 0,97 | 0,32 | 0,21 | 0,37 | 0,77 | 1,00 | | | | | | | | | | | | | | | | | | | | | | | |
| Y | -0,16 | -0,25 | -0,05 | 0,34 | 0,33 | 0,24 | -0,13 | -0,72 | -0,22 | -0,05 | 0,40 | 1,00 | | | | | | | | | | | | | | | | | | | | | | |
| Zr | 0,98 | 0,65 | 0,49 | 0,81 | 0,81 | 0,88 | 0,47 | 0,72 | 0,59 | 0,88 | 0,79 | -0,24 | 1,00 | | | | | | | | | | | | | | | | | | | | | |
| Nb | 0,61 | 0,92 | 0,95 | 0,85 | 0,58 | 0,82 | 0,90 | 0,61 | 0,91 | 0,96 | 0,70 | 0,10 | 0,70 | 1,00 | | | | | | | | | | | | | | | | | | | | |
| Mo | 0,61 | 0,94 | 0,94 | 0,83 | 0,55 | 0,80 | 0,93 | 0,65 | 0,93 | 0,96 | 0,67 | 0,05 | 0,71 | 1,00 | 1,00 | | | | | | | | | | | | | | | | | | | |
| Cd | -0,28 | 0,62 | 0,66 | -0,21 | -0,55 | -0,24 | 0,71 | 0,56 | 0,67 | 0,21 | -0,43 | -0,46 | -0,10 | 0,34 | 0,38 | 1,00 | | | | | | | | | | | | | | | | | | |
| In | -0,20 | 0,65 | 0,65 | -0,19 | -0,52 | -0,21 | 0,72 | 0,63 | 0,69 | 0,25 | -0,41 | -0,55 | -0,03 | 0,35 | 0,39 | 0,99 | 1,00 | | | | | | | | | | | | | | | | | |
| Sn | -0,28 | 0,63 | 0,67 | -0,19 | -0,54 | -0,23 | 0,72 | 0,54 | 0,68 | 0,22 | -0,42 | -0,44 | -0,11 | 0,36 | 0,39 | 0,99 | 0,99 | 1,00 | | | | | | | | | | | | | | | | |
| Sb | -0,31 | 0,61 | 0,64 | -0,22 | -0,57 | -0,26 | 0,70 | 0,53 | 0,66 | 0,19 | -0,45 | -0,45 | -0,13 | 0,33 | 0,36 | 0,99 | 0,99 | 0,99 | 1,00 | | | | | | | | | | | | | | | |
| Te | 0,57 | 0,92 | 0,80 | 0,44 | 0,21 | 0,48 | 0,83 | 0,98 | 0,90 | 0,80 | 0,27 | -0,59 | 0,71 | 0,74 | 0,78 | 0,62 | 0,68 | 0,62 | 0,60 | 1,00 | | | | | | | | | | | | | | |
| I | 0,18 | 0,52 | 0,36 | -0,19 | -0,32 | -0,12 | 0,44 | 0,86 | 0,52 | 0,27 | -0,32 | -0,94 | 0,31 | 0,17 | 0,22 | 0,70 | 0,77 | 0,68 | 0,68 | 0,78 | 1,00 | | | | | | | | | | | | | |
| Cs | 0,76 | 0,89 | 0,74 | 0,60 | 0,44 | 0,65 | 0,76 | 0,96 | 0,85 | 0,89 | 0,48 | -0,51 | 0,87 | 0,78 | 0,81 | 0,40 | 0,47 | 0,40 | 0,38 | 0,97 | 0,67 | 1,00 | | | | | | | | | | | | |
| Ba | 0,88 | 0,46 | 0,41 | 0,97 | 0,98 | 0,99 | 0,35 | 0,29 | 0,41 | 0,81 | 1,00 | 0,31 | 0,85 | 0,71 | 0,69 | -0,40 | -0,37 | -0,39 | -0,42 | 0,34 | -0,23 | 0,55 | 1,00 | | | | | | | | | | | |
| La | 0,45 | -0,17 | -0,42 | -0,15 | 0,12 | -0,02 | -0,37 | 0,39 | -0,24 | -0,05 | -0,04 | -0,72 | 0,40 | -0,32 | -0,29 | -0,28 | -0,17 | -0,30 | -0,29 | 0,20 | 0,49 | 0,29 | 0,03 | 1,00 | | | | | | | | | | |
| Ce | 0,43 | -0,03 | -0,27 | -0,18 | 0,02 | -0,05 | -0,22 | 0,54 | -0,08 | 0,02 | -0,11 | -0,85 | 0,42 | -0,24 | -0,20 | -0,07 | 0,03 | -0,10 | -0,09 | 0,36 | 0,66 | 0,41 | -0,03 | 0,98 | 1,00 | | | | | | | | | |
| Hf | -0,14 | 0,77 | 0,81 | 0,02 | -0,36 | -0,03 | 0,85 | 0,60 | 0,81 | 0,41 | -0,22 | -0,35 | 0,04 | 0,54 | 0,57 | 0,97 | 0,96 | 0,98 | 0,97 | 0,70 | 0,63 | 0,51 | -0,19 | -0,37 | -0,17 | 1,00 | | | | | | | | |
| Ta | 0,25 | 0,96 | 0,98 | 0,44 | 0,07 | 0,41 | 0,99 | 0,72 | 0,98 | 0,75 | 0,22 | -0,20 | 0,41 | 0,85 | 0,87 | 0,78 | 0,79 | 0,79 | 0,77 | 0,84 | 0,51 | 0,74 | 0,25 | -0,36 | -0,19 | 0,90 | 1,00 | | | | | | | |
| W | 0,22 | -0,30 | -0,53 | -0,40 | -0,13 | -0,27 | -0,47 | 0,29 | -0,35 | -0,26 | -0,29 | -0,77 | 0,17 | -0,51 | -0,47 | -0,18 | -0,09 | -0,21 | -0,20 | 0,09 | 0,52 | 0,13 | -0,22 | 0,97 | 0,98 | -0,33 | -0,43 | 1,00 | | | | | | |
| Hg | 0,77 | 0,53 | 0,53 | 0,99 | 0,93 | 0,98 | 0,46 | 0,24 | 0,49 | 0,83 | 0,98 | 0,44 | 0,76 | 0,80 | 0,77 | -0,29 | -0,28 | -0,28 | -0,31 | 0,33 | -0,30 | 0,51 | 0,97 | -0,19 | -0,24 | -0,07 | 0,36 | -0,43 | 1,00 | | | | | |
| Tl | 0,80 | 0,87 | 0,82 | 0,92 | 0,74 | 0,93 | 0,78 | 0,66 | 0,83 | 1,00 | 0,82 | 0,03 | 0,87 | 0,96 | 0,96 | 0,15 | 0,18 | 0,16 | 0,13 | 0,75 | 0,18 | 0,84 | 0,84 | -0,09 | -0,04 | 0,35 | 0,72 | -0,31 | 0,87 | 1,00 | | | | |
| Pb | -0,13 | 0,76 | 0,78 | -0,02 | -0,39 | -0,05 | 0,83 | 0,64 | 0,80 | 0,39 | -0,26 | -0,41 | 0,05 | 0,51 | 0,54 | 0,98 | 0,98 | 0,98 | 0,98 | 0,72 | 0,68 | 0,53 | -0,22 | -0,31 | -0,11 | 1,00 | 0,89 | -0,26 | -0,11 | 0,33 | 1,00 | | | |
| Bi | 0,20 | 0,95 | 0,97 | 0,40 | 0,02 | 0,36 | 0,99 | 0,71 | 0,97 | 0,72 | 0,17 | -0,21 | 0,37 | 0,83 | 0,84 | 0,81 | 0,81 | 0,82 | 0,80 | 0,83 | 0,52 | 0,72 | 0,20 | -0,37 | -0,20 | 0,92 | 1,00 | -0,43 | 0,32 | 0,69 | 0,91 | 1,00 | | |
| Th | 0,61 | 0,82 | 0,86 | 0,91 | 0,68 | 0,87 | 0,81 | 0,45 | 0,81 | 0,93 | 0,79 | 0,29 | 0,68 | 0,98 | 0,97 | 0,18 | 0,17 | 0,20 | 0,16 | 0,59 | -0,03 | 0,66 | 0,79 | -0,40 | -0,36 | 0,40 | 0,74 | -0,60 | 0,89 | 0,95 | 0,36 | 0,71 | 1,00 | |
| U | 0,23 | 0,96 | 0,98 | 0,43 | 0,06 | 0,39 | 0,99 | 0,71 | 0,98 | 0,74 | 0,20 | -0,20 | 0,40 | 0,84 | 0,86 | 0,79 | 0,80 | 0,80 | 0,78 | 0,84 | 0,51 | 0,73 | 0,23 | -0,37 | -0,19 | 0,91 | 1,00 | -0,43 | 0,35 | 0,71 | 0,89 | 1,00 | 0,73 | 1,00 |

**Table 3:** Comparison of Sb ore and granitoid trace elements.

| Elements | Average values of Üçkapılı granitoid (Kurt et al., 2013) | Average of this work | |
|---|---|---|---|
| Cu | 6.20 | 20.47 | Increase in ore |
| Pb | 2.14 | 65.62 | |
| Sr | 135.58 | 457.65 | |
| Ba | 538.53 | 35553.78 | |
| Ta | 1.03 | 8.20 | |
| Cs | 3.10 | 69.92 | |
| Zn | 44.71 | 29.77 | Increase in rock |
| Ga | 17.42 | 4.65 | |
| Rb | 106.84 | 9.3 | |
| Th | 11.70 | 1.92 | |
| Nb | 13.64 | 9.30 | |
| Zr | 152.34 | 4.87 | |
| Y | 31.86 | | |

**Acknowledgement**
This study is supported by Nigde Omer Halisdemir University Scientific Research Projects Coordination Unit with the Project number of FEB 2017/22-BAGEP.

**References**

[1]. Özen, Y. and Arık. (2016). Mineralogy, Geochemistry and Stable Isotope Investigation of Gürkuyu Sb Mineralization (Gediz-Kütahya-NW Turkey). Cumhuriyet University Faculty of Science Science Journal (CSJ), Vol. 37. 738-748
[2]. Janković S. (1997). The Carpatho–Balkanides and adjacent area: a sector of the Tethyan Eurasian metallogenic belt, Miner Deposita 32, 426–433.
[3]. Power-Fardy D., Magaranov G. (2013). A technical review of the Borsko Jezero copper- gold property, Bor, Serbia for Mundoro Capital Inc., Watts, Griffis and McOuat Limited, Toronto, Canada, 74 pp.
[4]. Akçay, M. (1995). Geological and mineralogical investigation of the Gümüşler (Niğde) Sb±Hg±W occurences and implications on their gold potential. Geological Bulletin of Turkey, V. 38, No. 2, 23-34.
[5]. Dennis, R.A., (1970). The Mineralization at the Hg-Sb-W Mine near Niğde, South-Central Turkey: Master tezi, Swansea University, (Unpublished).
[6]. Yıldız, M., (1978). Türkiye'de Bazı Civa Yataklarının Oluşum ve Mukayesesi: MTA Yayın No: 173, Ankara.
[7]. Göncüoğlu, M. C., V. Toprak, I. Kuşçu, A. Erler, and E. Olgun (1991). Orta Anadolu Masifinin batı bölümünün jeolojisi, Bölüm1: Güney Kesim, Turkish Petroleum Corporation (TPAO) Report, 2909, 140 pp.
[8]. Göncüoğlu, M.C., (1981). The Origin of Viridine–gneiss from Niğde Massif. Bulletion of the Geological Society of Turkey, V. 24, 45-51, February.
[9]. Göncüoğlu, M.C., (1982). Zircon U/Pb ages from paragneisses of the Niğde Massif (Central Anatolia). Bulletin of the Geological Society of Turkey, V. 25, 61 - 66, February, 1982.
[10]. Whitney, D. L., and Y. Dilek (1998). Metamorphism during Alpine crustal thickening and extension in Central Anatolia, Turkey: The Niğde metamorphic core complex, J. Petrol., 39, 1385 – 1403.
[11]. Whitney DL, Teyssier C, Heizler MT (2007). Gneiss domes, metamorphic core complexes, and wrench zones: thermal and structural evolution of the Niğde Massif, central Anatolia. Tectonics 26: TC5002.

[12]. Gautier, P., Bosse, V., Hallot, E. and Dirik, K. (2008). Coeval extensional shearing and lateral underflow during Late Cretaceous core complex development in the Nigde Massif, Central Anatolia, Turkey. Tectonophysic, 27, 1-27.

[13]. Kuscu, I., and Erler, A. (1999). Deformation of Stibnites and Pyrites in the Madsan Antimony Deposit (Nigde, Turkey): Implications for Pressure-Temperature Conditions of Local Deformation. Turkish Journal of Earth Sciences 8, 57-66.

[14]. Akçay, M., Moon, C. J., and Scott, B. C. (1995). Mineralchemie und Flüssigkeitseinchlüsse der bei der Sb-Hg± W-lagerstatte auftretenden Turmaline im Gebiet Gümüşler (Niğde Massive, Zentral-Türkei). Chem. Erde., 55, 225-236.

[15]. Yalçın, F; Tumuklu, A; Boztas, S. Ilbeyli, N; (2016). Investigation Of Statistical Relationships Between Au, Ag, As, Ba, Cd, Cu, Fe, Pb, S, Sb, And Zn Elements Of Antimony Deposit In NW Camardı–Nıgde (Turkey). 16th International Multidisciplinary Scientific GeoConference SGEM, Albena, BULGARIA, 28th June - 7th July 2016.

[16]. Tümüklü, A. (2013). Gümüşler (Niğde) Bölgesinde Toprakta ve Suda Bulunan Arseniğin Kaynak Kayaçlarının Araştırılması. 2. Tıbbi Jeoloji Çalıştayı. 4-6 Aralık 2013. Antalya. s: 335-336.

[17]. Tümüklü, A. And Yalçın, M. G., (2016). Economic And Environmental Effects Of Historical Mining Enterprises In Gumuşler Village And Çamardı Towns Region (NIGDE, TURKEY). 16th International Multidisciplinary Scientific GeoConference SGEM, Albena, BULGARIA, 28th June - 7th July.

[18]. Whitney, D. L., Teyssier, C., Fayon, A. K., Hamilton, M. A., Heizler M. (2003). Tectonic controls on metamorphism, partial melting, and intrusion: Timing and duration of regional metamorphism and magmatism in the Nigde Massif, Turkey. Tectonophysics 376, 37 – 60.

[19]. Kurt, H., Koçak, K., Asan, K., and Karakaş, M. (2013). Petrogenesis of the Üçkapılı Granitoid and its enclaves in Elmalı area (Niğde, Central Anatolia, Turkey). Acta Geologica Sinica (English Edition). Vol: 87. No. 3. Pp: 738-748.

[20]. Göncüoglu, M.C. (1986). Geochronologic data from the southern part (Nigde area) of the Central Anatolian Massif. Mineral Research and Exploration Institute of Turkey (MTA) Bulletin 105/106, 83-96 [in Turkish with English abstract].

[21]. Dill, H. G. (2010). The "chessboard" classification scheme of mineral deposits: mineralogy and geology from aluminum to zirconium. Earth-Science Reviews 100, 1-420.

[22]. Lindgren, W. (1933). Mineral deposits, 4th ed., Mc Graw Hill, NewYork, 930 p.

[23]. Göncüoğlu, M.C., Erler, A., Toprak, G.M.V., Yalınız, K., Olgun, E., and Rojay, B., (1992). Orta Anadolu Masifinin batı bölümünün jeolojisi, Bölüm 2: Orta kesim: O.D.T.Ü.- AGUDÖS Rep., 76 p., (unpublished).

[24]. Alpar, C. R. (2011). Çok değişkenli İstatiksel Yöntemler. Detay Yayıncılık, Ankara.